



# Inhibition of the NKCC1/NF- $\kappa$ B Signaling Pathway Decreases Inflammation and Improves Brain Edema and Nerve Cell Apoptosis in an SBI Rat Model

Yating Gong<sup>1</sup>, Muyao Wu<sup>1</sup>, Jinchao Shen<sup>2</sup>, Jiafeng Tang<sup>1</sup>, Jie Li<sup>3</sup>, Jianguo Xu<sup>4\*</sup>, Baoqi Dang<sup>1\*</sup> and Gang Chen<sup>5</sup>

<sup>1</sup> Department of Rehabilitation, Zhangjiagang TCM Hospital Affiliated to Nanjing University of Chinese Medicine, Suzhou, China, <sup>2</sup> Department of Anesthesiology, Zhangjiagang TCM Hospital Affiliated to Nanjing University of Chinese Medicine, Suzhou, China, <sup>3</sup> Department of Intensive Care Unit, Zhangjiagang TCM Hospital Affiliated to Nanjing University of Chinese Medicine, Suzhou, China, <sup>4</sup> Department of Neurosurgery, The First Affiliated Hospital of Soochow University, Suzhou, China, <sup>5</sup> Department of Neurosurgery and Brain and Nerve Research Laboratory, The First Affiliated Hospital of Soochow University, Suzhou, China

## OPEN ACCESS

### Edited by:

Jong Eun Lee,  
Yonsei University, South Korea

### Reviewed by:

Tiziano Balzano,  
Centro Integral en Neurociencias A.C.  
HM CINAC, Spain  
Li Tian,  
University of Tartu, Estonia

### \*Correspondence:

Baoqi Dang  
zhenjiangdbq@163.com  
Jianguo Xu  
xejianlov2012@gmail.com

Received: 15 December 2020

Accepted: 08 March 2021

Published: 31 March 2021

### Citation:

Gong Y, Wu M, Shen J, Tang J, Li J, Xu J, Dang B and Chen G (2021) Inhibition of the NKCC1/NF- $\kappa$ B Signaling Pathway Decreases Inflammation and Improves Brain Edema and Nerve Cell Apoptosis in an SBI Rat Model. *Front. Mol. Neurosci.* 14:641993. doi: 10.3389/fnmol.2021.641993

Surgical brain injury (SBI) triggers microglia to release numerous inflammatory factors, leading to brain edema and neurological dysfunction. Reducing neuroinflammation and protecting the blood-brain barrier (BBB) are key factors to improve the neurological function and prognosis after SBI. Na<sup>+</sup>-K<sup>+</sup>-Cl<sup>-</sup> cotransporter 1 (NKCC1) and nuclear factor  $\kappa$ B (NF- $\kappa$ B) have been implicated in the secretion of inflammatory cytokines by microglia in brain injury. This study aimed to establish the role of NKCC1 in inducing inflammation in SBI, as well as to determine whether NKCC1 controls the release of interleukin-1 $\beta$  (IL-1 $\beta$ ), interleukin-6 (IL-6), and tumor necrosis factor- $\alpha$  (TNF- $\alpha$ ) via phosphorylation of NF- $\kappa$ B in microglia, thus affecting BBB permeability and neuronal cell apoptosis. Male Sprague-Dawley (SD) rats were used to establish an SBI model. This study revealed that compared with the sham group, the expression levels of p-NKCC1, p-p65-NF- $\kappa$ B, and related inflammatory factor proteins in SBI model group significantly increased. After p-NKCC1 was inhibited, p-p65-NF- $\kappa$ B, IL-6, IL-1 $\beta$ , and TNF- $\alpha$  were downregulated, and nerve cell apoptosis and BBB permeability were significantly reduced. These findings suggest that the SBI-induced increase in p-NKCC1 exacerbates neuroinflammation, brain edema, and nerve function injury, which may be mediated by regulating the activity of p65-NF- $\kappa$ B that in turn influences the release of inflammatory factors.

**Keywords:** surgical brain injury, NKCC1, NF- $\kappa$ B, neuroinflammation, brain edema, apoptosis

## INTRODUCTION

Brain surgery plays a major role in studying the etiology and treatment of brain diseases (Hamard et al., 2016). At the same time, due to incision, electrocoagulation, bleeding, and other invasive operations in the process of brain surgery, there will be some damage to the brain tissue around the operation site, which is called surgical brain injury (SBI) (Akyol et al., 2018). Studies have shown that nearly one-fifth of patients experience serious complications after craniocerebral operation (Sherchan et al., 2016). After brain injury caused by various reasons, immune cells are activated, triggering the release of pro-inflammatory cytokines, thus resulting in the formation of an inflammatory environment in the brain, which is a feature of many brain pathologies. When inflammatory signals are activated, multiple cell signals in the brain change, which may eventually lead to neurological dysfunction and cell apoptosis (Lima Giacobbo et al., 2019). Neuroinflammation is a major adverse reaction that occurs after brain injury that may lead to brain edema, nerve cell apoptosis, as well as aggravated nerve function injury (Xiao et al., 2018). Microglia cells pertain to immune cells in the central nervous system. Generally, microglia are at rest. In brain injury, microglia are stimulated to activate the nuclear factor  $\kappa$ B (NF- $\kappa$ B) signaling pathway, which induces cells to contribute to the generation of an inflammatory response and triggers microglia to secrete a various inflammatory factors, including interleukin-1 $\beta$  (IL-1 $\beta$ ), interleukin-6 (IL-6), as well as tumor necrosis factor alpha (TNF- $\alpha$ ), which then cause cellular neurotoxicity and lead to secondary brain injury (Wu et al., 2017b; Zhang et al., 2020a).

Previous studies have shown that inflammation can worsen brain edema (Adukauskiene et al., 2007). After brain injury, inflammatory cytokines such as IL-1 $\beta$ , IL-6, TNF- $\alpha$ , as well as oxidative stress mediators are upregulated, which then may result in apoptosis of large neurons and incur blood-brain barrier (BBB) damage, thereby exacerbating brain edema and nerve cell damage (Chen et al., 2014; Zhang et al., 2020b). Inflammation can increase cell permeability, disrupt the BBB, and lead to vasogenic brain edema; it also causes cell degeneration and apoptosis, and if necrotic and apoptotic cells are not immediately consumed by phagocytes, then these could release toxic signals to surrounding cells, leading to cytotoxic brain edema (Sherchan et al., 2017; Xiao et al., 2018).

Na<sup>+</sup>-K<sup>+</sup>-Cl<sup>-</sup> cotransporter 1 (NKCC1) is expressed in glial cells, neurons, endothelial cells, and choroid plexus epithelial cells (Simard et al., 2010). The primary function of NKCC1 is to regulate the entry of Na<sup>+</sup>, K<sup>+</sup>, Cl<sup>-</sup>, and water into cells to regulate the transfer and invasion of inflammatory mediators and other related factors, which can lead to brain edema, inflammation, and secondary brain damage. NKCC1 is closely related to cerebral hemorrhage (Wu et al., 2020a), stroke (Wu et al., 2020b), epilepsy (Gharaylou et al., 2019; Zhang et al., 2020b), traumatic brain injury (Sudhakar et al., 2019), and other brain diseases. However, the activity of NKCC1 is mainly regulated by the STE20-related proline/alanine kinase (SPAK)/oxidative stress response 1 (OSR1) signaling pathway. After injury, SPAK/OSR1 is activated to phosphorylate downstream NKCC1 (Yan and Merlin, 2008). SPAK/OSR1, which is the upstream kinase of

NKCC1, binds to NKCC1 through its conserved C-terminal domain, phosphorylates Thr203, Thr207, and Thr212 residues on NKCC1, thus promoting the increase of inflammatory cells and aggravating the inflammatory response after injury (Reid et al., 2013; Hung et al., 2020). Inhibition of NKCC1 downregulates the expression of intracellular NF- $\kappa$ B phosphorylation (Zhang et al., 2017), thus reducing the activation of inflammatory cells and cell volume-related functions and decreasing brain edema and nerve cell injury after brain injury (Hung et al., 2018; Gomez et al., 2019). Pro-inflammatory cytokines IL-1 $\beta$ , IL-6, and TNF- $\alpha$  also play an important role in the inflammatory response via this signaling pathway.

Neuroinflammation induced by SBI surgery can aggravate brain edema and postoperative nerve function injury (Huang et al., 2020a). Currently, the treatment of secondary brain injury after SBI is limited. Therefore, the development of endogenous therapeutic measures will be a safe way to reduce postoperative complications of SBI. Bumetanide (BUM) is a loop diuretic that acts by inhibiting NKCC1 and NKCC2. NKCC1 is expressed in the central nervous system and systemic organs, and BUM regulates the transmembrane Cl<sup>-</sup> gradient of neurons by blocking NKCC1 (Kharod et al., 2019). BUM was proposed to provide an interesting therapeutic option for such brain diseases by reducing intraneuronal Cl<sup>-</sup> levels and restoring GABAergic inhibition (Hampel et al., 2021). Currently, BUM has been proposed to inhibit NKCC1 to reduce intracranial Cl<sup>-</sup> level, providing a treatment option for this kind of brain disease. BUM was identified and recognized nearly 40 years ago and has been used to treat hypertension and brain edema, with side effects limited to diuretics, hypokalemia and dehydration (Ben-Ari, 2017). The aim of this study was to investigate the relationship between NKCC1 and microglia cell-induced release of inflammatory factors after SBI, as the inhibition of NKCC1 can reduce p-p65-NF- $\kappa$ B activation, decrease the release of inflammatory factors, thereby reducing brain edema and nerve cell apoptosis as well as improving nerve function, indicating that it plays a role in brain protection.

## MATERIALS AND METHODS

### Experiment Design and Grouping

Experiment 1: No significant difference in weight, exercise ability, and food intake were observed among groups. Time course analysis of NKCC1 and p-NKCC1 protein levels in 28 rats after SBI. A total of 28 rats (all survived) were randomly assigned to one of seven groups ( $n = 4$  per group), namely, the sham operation group, and six experimental groups that were arranged in chronological order of 6 h, 12 h, 24 h, 48 h, 72 h, and 7 days post SBI operation. The rats were sacrificed at a time between 6 h and 7 days, which was 36 h after sham surgery. The brain tissue around the damaged area in each rat was collected. Western blotting (WB) of a portion of the brain tissues was conducted to determine the expression of NKCC1 and p-NKCC1, and the rest of the tissue samples was used for double immunofluorescence (IF) to assess the expression of p-NKCC1 (Figure 1C).

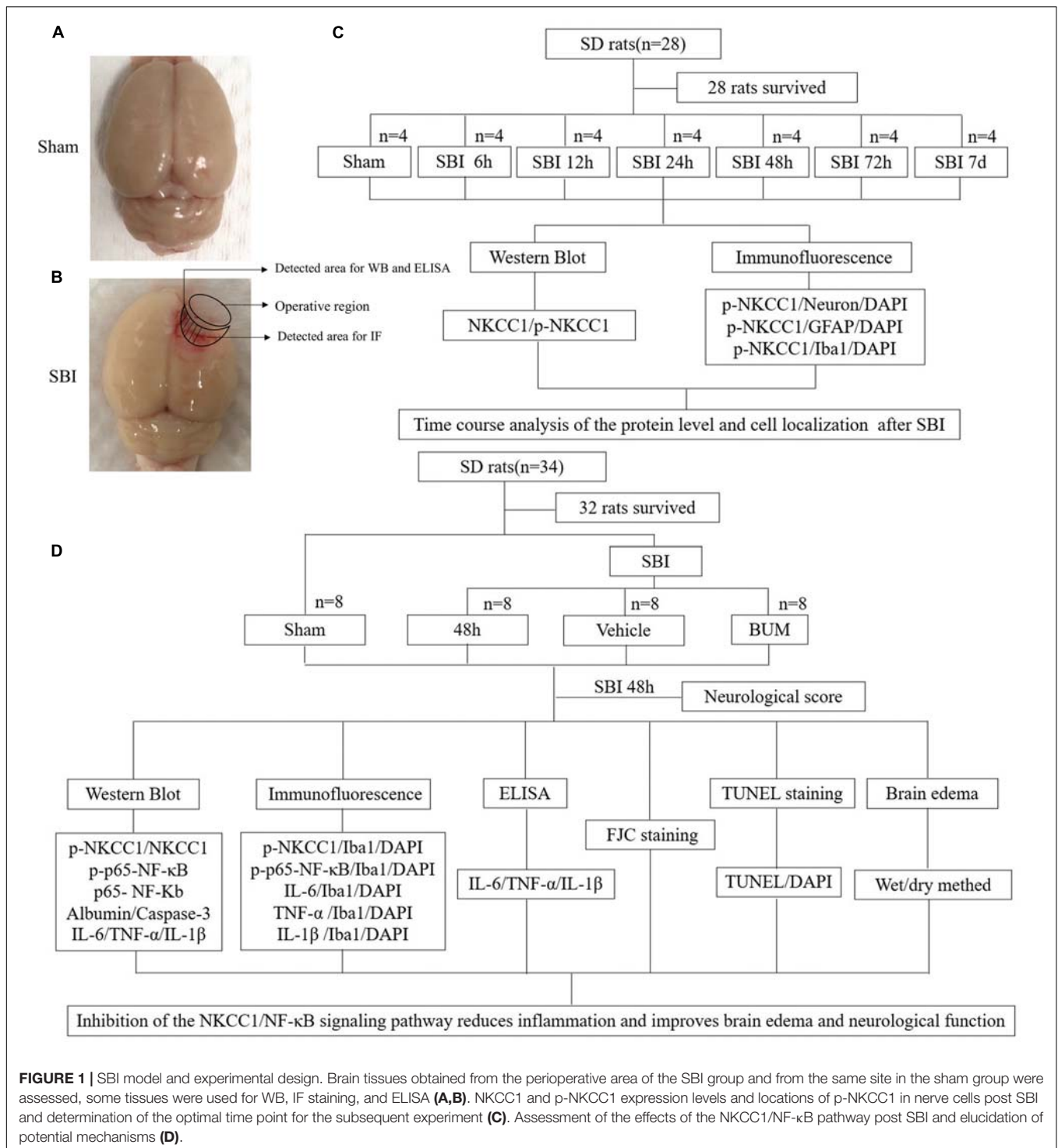


**FIGURE 1** | SBI model and experimental design. Brain tissues obtained from the perioperative area of the SBI group and from the same site in the sham group were assessed, some tissues were used for WB, IF staining, and ELISA (A,B). NKCC1 and p-NKCC1 expression levels and locations of p-NKCC1 in nerve cells post SBI and determination of the optimal time point for the subsequent experiment (C). Assessment of the effects of the NKCC1/NF- $\kappa$ B pathway post SBI and elucidation of potential mechanisms (D).

Experiment 2: To determine the role of p-NKCC1 in SBI, 32 rats (a total of 34 rats were used, of which 32 survived) were randomly assigned to one of the four groups, namely, sham, SBI, SBI + vehicle, and SBI + BUM. Based on the results of experiment 1, the rats were sacrificed 48 h post SBI, and brain tissues surrounding the damaged area were collected. Neurological examination of all groups was performed prior

to death. Sixteen rats (four rats per group) were used in WB, IF, and enzyme-linked immunosorbent assay (ELISA). Brain tissues near the pre-lesion area were used in WB to determine p-NKCC1, p-p65-NF- $\kappa$ B, p65-NF- $\kappa$ B, albumin, caspase-3, IL-1 $\beta$ , IL-6, and TNF- $\alpha$  expression and in ELISA for IL-1 $\beta$ , IL-6, TNF- $\alpha$  expression. Tissues in the post-lesion area were processed for paraffin sectioning for TdT-mediated dUTP nick-end labeling

(TUNEL) staining as well as Fluoro-Jade C (FJC) to assess nerve cell apoptosis and necrosis. Sixteen rats (four in each group) were evaluated for brain edema. The experiment was conducted with blinded experimenters (Figure 1D).

## Experimental Animals

All experiments received approval from the Institute of Animal Care Committee of Zhangjiagang Traditional Chinese Medicine Hospital (Zhangjiagang, China) and were conducted following the guidelines on the care and use of animals of the National Institutes of Health. We purchased male Sprague-Dawley (SD) rats (age: 8 weeks; weight: 320–350 g) from the Zhaoyan (Suzhou) New Drug Research Center. The rats were maintained under constant temperature and relative humidity, as well as were fed using a regular light/dark cycle. Food and water were provided *ad libitum*.

## Establishment of Experimental Rat SBI Model

A rat SBI model was used as earlier reported (Huang et al., 2020a). SD rats were anesthetized via intraperitoneal injection of sodium pentobarbital (40 mg/kg). The rats were then placed in a prone position and fixed onto a stereotaxic apparatus (Yuyan, China). An incision was made along the midline of the skin above the brain to expose the skull to identify the bregma. Then, a 5 mm  $\times$  5 mm craniotomy was performed on the right frontal skull and removed with a bone drill on the right skull bone 2 mm along the sagittal suture and 1 mm along coronal suture. A durotomy was performed, and 2 mm  $\times$  3 mm brain tissue was excised by sharp dissection (Yang et al., 2016). An electrocautery unit was used to stop bleeding, then the area was rinsed with normal saline. In the sham rats, the same surgical method was used; craniotomy was performed to remove the bone flap, but part of the right frontal lobe was not removed. Important parameters of interest were monitored during and after surgery. The rats were sacrificed at different time points according to experimental requirements.

## Drug Injection

The rats were randomly assigned into one of four groups, namely, Sham, SBI, SBI + vehicle, and SBI + BUM (15 mg/kg, 10% DMSO); rats in the SBI + BUM were treated via tail vein injection 15 min before SBI (Lu et al., 2006). The weight-matched SBI + vehicle group was injected with 10% equal volume of DMSO.

## Tissue Collection and Sectioning

The rats were anesthetized with sodium pentobarbital via intraperitoneal injection at 48 h post SBI (Figures 1A,B). To isolate proteins, the rats were perfused with 0.9% normal saline (200 mL, 4°C) through the heart, and cortical samples <3 mm from the contusion edge were collected on ice. Some tissue samples were flash frozen and stored at  $-80^{\circ}\text{C}$  until analysis by WB and ELISA. To obtain brain sections, brains were harvested, fixed in 4% paraformaldehyde for >48 h at 4°C, followed by paraffin embedding. Paraffin brain sections were sectioned using a microslicer with a thickness of 5  $\mu\text{m}$  each

(Wu et al., 2020c). Tissue removal and selection were conducted by two blinded pathologists.

## WB Analysis

Western blotting (WB) analysis was performed as previously described (Tsai et al., 2020). The extracted brain tissue was homogenized in tissue protein extraction reagent with protease inhibitor cocktail (CW BIO, China) and incubated on ice for 20 min. Then, the homogenate was centrifuged at 12,000 g for 20 min at 4°C. The supernatant was collected, then the bicinchoninic acid (BCA) method and the Pierce<sup>TM</sup> BCA protein detection kit (Thermo Fisher Scientific, United States) were employed to determine total protein concentration. Equal amounts of the extracted proteins were loaded and resolved by electrophoresis on a TGX Stain-Free FastCast Acrylamide Kit (Bio-Rad, United States), and then transferred onto a PVDF membrane (Millipore, United States). QuickBlock<sup>TM</sup> Western (Beyotime, China) was employed to block the PVDF membrane at room temperature for 30 min and then sealed for 30 min at room temperature. The sections were then incubated with primary antibodies in a refrigerated shaker at 4°C overnight. The antibodies used were mouse anti-NKCC1 (Santa Cruz, CA, United States), rabbit anti-p-NKCC1 (Sigma, United States), rabbit anti-Albumin (Abcam, United Kingdom), rabbit anti-p-p65-NF- $\kappa$ B (Abcam), rabbit anti-p65-NF- $\kappa$ B (Abcam), rabbit anti-IL-1 $\beta$  (Abcam), rabbit anti-IL-6 (Abcam), and rabbit anti-TNF- $\alpha$  (Abcam), rabbit anti-caspase-3 (Abcam); Rabbit anti-GAPDH (Sigma) was used as internal loading control. After washing PBS thrice, the sections were incubated with secondary antibodies, which included anti-mouse IgG, HRP (Cell Signaling, United States), and anti-rabbit IgG-HRP (Invitrogen, United States) for 2 h at 4°C. The immunoblots were then stained with Immobilon<sup>®</sup> Western Chemiluminescent HRP Substrate (Millipore, United States) and visualized using an imaging system (GE Healthcare Bio-Sciences AB, Sweden). The data were analyzed by ImageJ software (National Institutes of Health, MD, United States).

## Immunofluorescence Staining

Double IF staining was performed as earlier described (Zhao et al., 2016). A paraffin section oven was set at 70°C for 1 h. After soaking in xylene, anhydrous ethanol, 95%, 85%, and 70% ethanol, sodium citrate was used for repair. Then, the sections were washed thrice with phosphate-buffered physiological saline (PBS) after the membrane was permeabilized using an immunostaining permeable solution (Beyotime, China). The brain sections were blocked for at least 30 min in a blocking solution, then incubated with the indicated primary antibody at 4°C overnight. After three PBS washes, the sections were incubated with a secondary antibody at room temperature for 1 h. Finally, the tablets were sealed with DAPI anti-fluorescence quenching solution (YEASEN, China) and observed under a fluorescence microscope (OLYMPUS, Japan). Antibodies: rabbit anti-p-NKCC1 (Sigma, United States), rabbit anti-p-p65-NF- $\kappa$ B (Abcam), rabbit anti-NF- $\kappa$ B (Abcam), rabbit anti-IL-1 $\beta$  (Abcam), rabbit anti-IL-6 (Abcam), and rabbit anti-TNF- $\alpha$  (Abcam), mouse anti-GFAP (Invitrogen, United States), goat anti-Iba1



(Abcam), mouse anti-NeuN (Abcam), donkey anti-rabbit IgG antibody, Alexa Fluor 488 (Invitrogen), donkey anti-mouse IgG antibody, Alexa Fluor 555 (Invitrogen), donkey anti-goat IgG antibody, Alexa Fluor 555 (Invitrogen).

## Neurological Score

Neurological scoring was conducted as previously described (Feng et al., 2017) and consisted of the following seven components: (1) symmetry of limb movement; (2) forelimb-stretching exercises; (3) lateral turning; (4) climbing; (5) body movements; (6) responses to vibrissae touch; and (7) proprioception. Scores on each subtest ranged from 0 to 3, with a combined maximum score of 21. Higher scores were indicative of less neurological damage.

## ELISA

Interleukin-1 $\beta$  (IL-1 $\beta$ ), IL-6, and TNF- $\alpha$  expression levels around the damaged rats brain areas were assessed by ELISA with a rat IL-1 $\beta$ , IL-6, TNF- $\alpha$  kit (BOSTER, China). This assay was conducted following the manufacturer's instructions, and the collected data were expressed relative to a generated standard curve of IL-1 $\beta$ , IL-6, and TNF- $\alpha$ .

## TUNEL Staining

Apoptosis was determined via TUNEL staining following the manufacturer's protocol (Beyotime, China). The paraffin-section dewaxing steps were the same as those described above. The samples were washed with distilled water for 2 min, followed by incubation for 30 min in a protease-K working solution. Later, the samples were washed thrice with PBS (5 min each wash). The brain sections were overlaid with TUNEL working solution and then incubated in a humidified box at 37°C for 1 h in the dark. The samples were then washed thrice with PBS (5 min each wash) and sealed with DAPI anti-fluorescence quenching solution (YEASEN, China).

## FJC Staining

Fluoro-Jade C staining was conducted following the manufacturer's instructions (Biosensis, United States). The samples were incubated in a paraffin section oven at 70°C for 1 h. Then, the samples were successively soaked in xylene, 100% ethanol, and 70% ethanol. Subsequently, the samples were washed twice with double-distilled H<sub>2</sub>O (1 min each time) followed by washing with distilled water for 2 min. Then, nine parts of distilled water were mixed with one part of solution B (potassium permanganate); the slides were then incubated for 10 min. Thereafter, slides were washed with distilled water for 2 min. Then, nine parts of distilled water were mixed with one part of solution C, and the samples were incubated in the dark for 10 min. After washing thrice with distilled water, the samples were dried in a 60°C oven for at least 5 min. Then, the samples were soaked in xylene for 5 min. After drying, the samples were sealed with neutral resin in liquid (YEASEN) and observed under a fluorescent microscope.

## Brain Edema

Brain edema was assessed, and brain moisture content was assessed using the wet-dry method. After separating the rat brain tissues, these were sectioned into symmetrical sides and their wet weights were immediately determined. Then, the brain samples were dried in a 100°C oven for 24 h, followed by dry weight determination. Brain water content (%) was estimated as follows: [(Wet weight - Dry weight) / (Wet weight)]  $\times$  100% (Wang et al., 2015).

## Statistical Analyses

All data are expressed as the mean  $\pm$  standard deviation (SD). Statistical analysis was performed using GraphPad Prism 8.0 software. K-W One-way ANOVA for multiple comparisons as well as Student-Newman-Keuls *post hoc* tests were employed to determine significant differences among study groups. Differences with a  $P < 0.05$  were considered statistically significant.

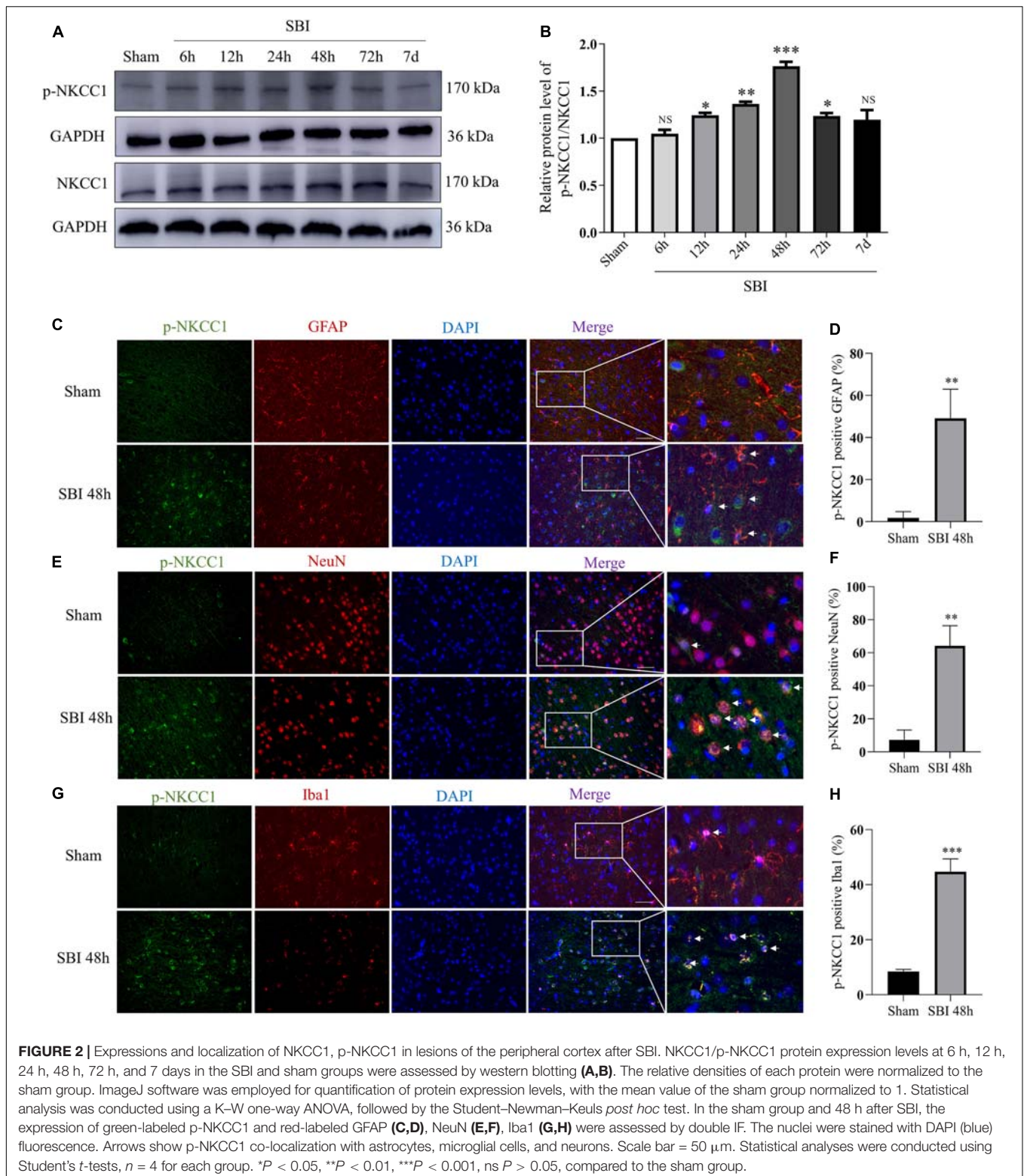
## RESULTS

### Changes and Localization of NKCC1 and p-NKCC1 Protein Expression Levels in the SBI Brain

Na<sup>+</sup>-K<sup>+</sup>-Cl<sup>-</sup> cotransporter 1 (NKCC1) and p-NKCC1 expression levels were assessed at 6 h, 12 h, 24 h, 48 h, 72 h, and 7 days in the SBI and sham groups by WB and the changes of p-NKCC1 in cortical cells before and after SBI (**Figure 2**). p-NKCC1 expression began to rise 12 h after SBI and peaked at 48 h. After 48 h, protein levels and p-nkcc1 decreased. By 7 days, protein expressions levels returned back to normal, whereas that of NKCC1 did not change (**Figures 2A,B**). P-NKCC1 expression was evaluated by IF staining of GFAP, NeuN, and Iba1. The analysis showed that the number of p-NKCC1-positive astrocytes (**Figures 2C,D**), neurons (**Figures 2E,F**), and microglia (**Figures 2G,H**), were higher at 48 h in the SBI group relative to the sham group.

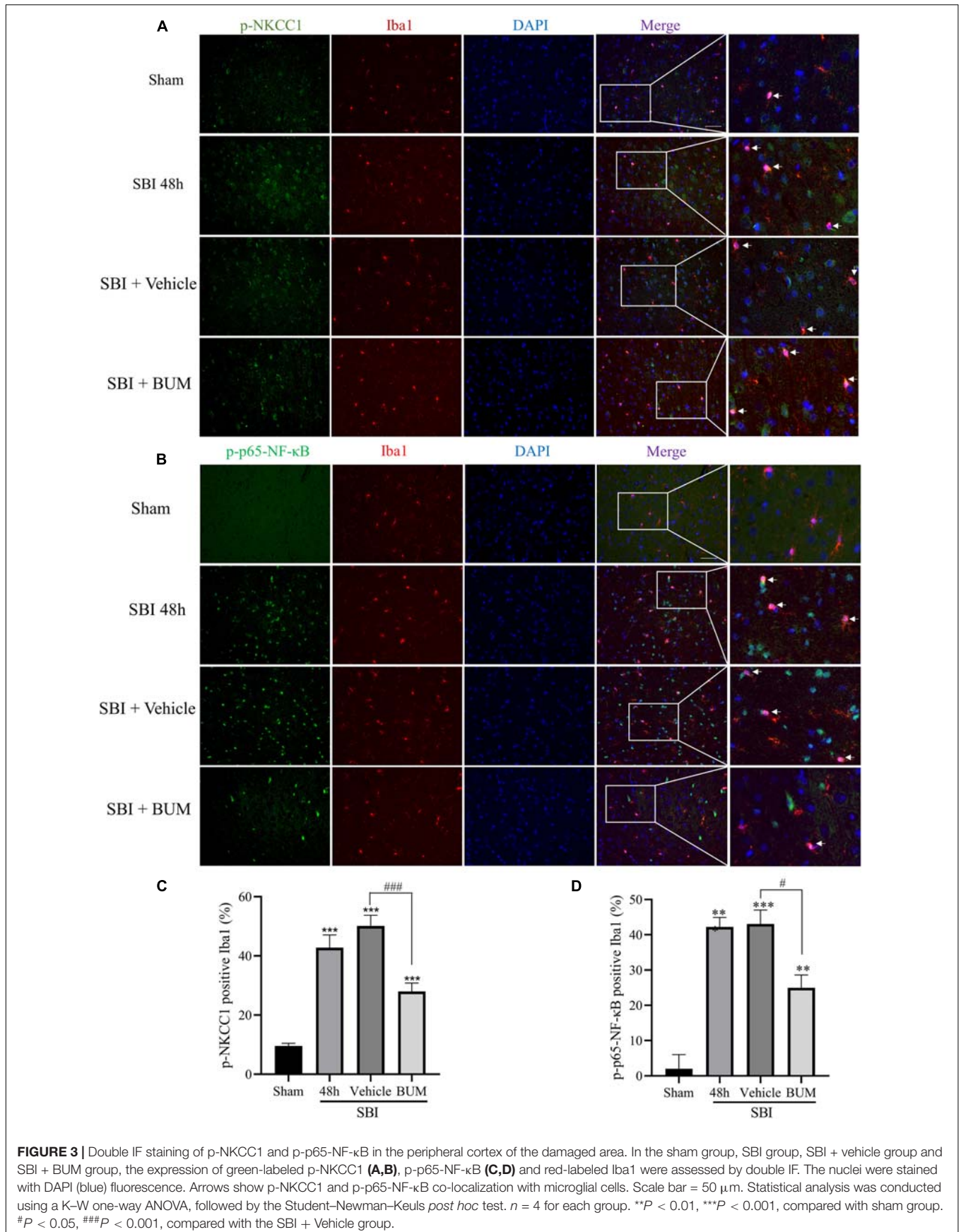
### Effects of BUM Intervention on NKCC1/NF- $\kappa$ B Signaling Pathway and Inflammatory Cytokines in Microglia After SBI

Compared with sham group, the expressions of p-NKCC1 and p-p65-NF- $\kappa$ B in microglia of the SBI group, SBI + vehicle group, and SBI + BUM group were significantly increased. After BUM intervention, the expressions of p-NKCC1 and p-p65-NF- $\kappa$ B in microglia in the SBI + BUM group were decreased compared with the SBI + vehicle group (**Figures 3A-D**). Compared with sham group, the expression of TNF- $\alpha$  in the SBI group, SBI + vehicle group, and SBI + BUM group were significantly increased. After BUM intervention, TNF- $\alpha$  in microglia of the SBI + BUM group was not significantly changed compared with that of the SBI + vehicle group (**Figures 4E,F**). The variation trend of IL-1 $\beta$  (**Figures 4A,B**) and IL-6 (**Figures 4C,D**)

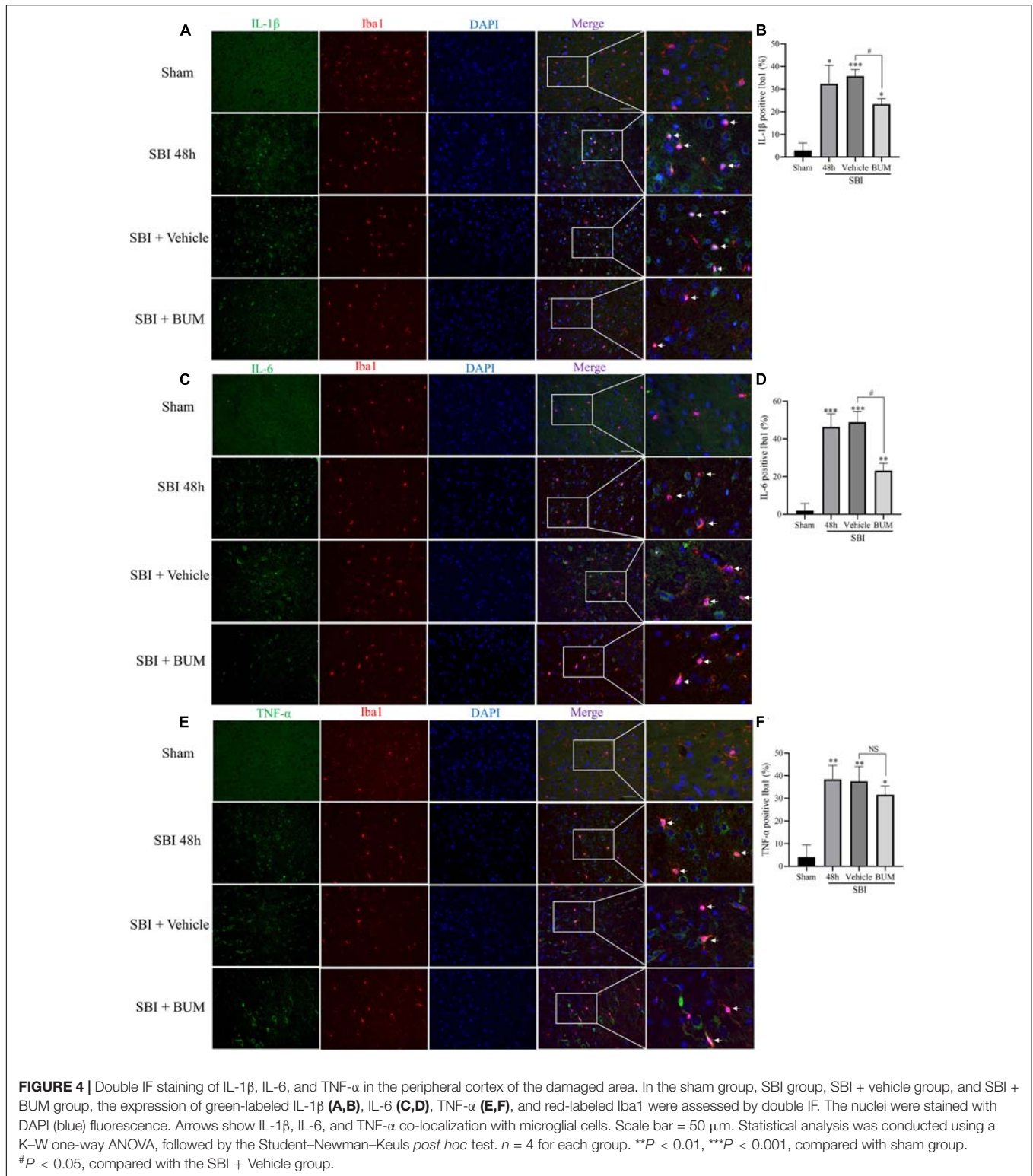


in microglia was basically consistent with that of p-NKCC1/p-p65-NF- $\kappa$ B. These results confirmed that the increase of p-NKCC1 and p-p65-NF- $\kappa$ B in microglia of SBI stimulated the release of a large number of inflammatory cytokines from

microglia, and BUM intervention could alleviate this process. These results confirmed that a large number of inflammatory cytokines were released after SBI. BUM intervention can alleviate this process.







## BUM Intervention on the Expression of Cortical Related Proteins After SBI

Compared with the sham group, p-NKCC1, and p-p65-NF- $\kappa$ B expression markedly increased in the SBI group, SBI +

vehicle group, and SBI + BUM group. After BUM intervention, WB showed that compared with the SBI + vehicle group, p-NKCC1, and p-p65-NF- $\kappa$ B expression in the SBI + BUM group decreased (Figures 5A–D). Compared with the sham



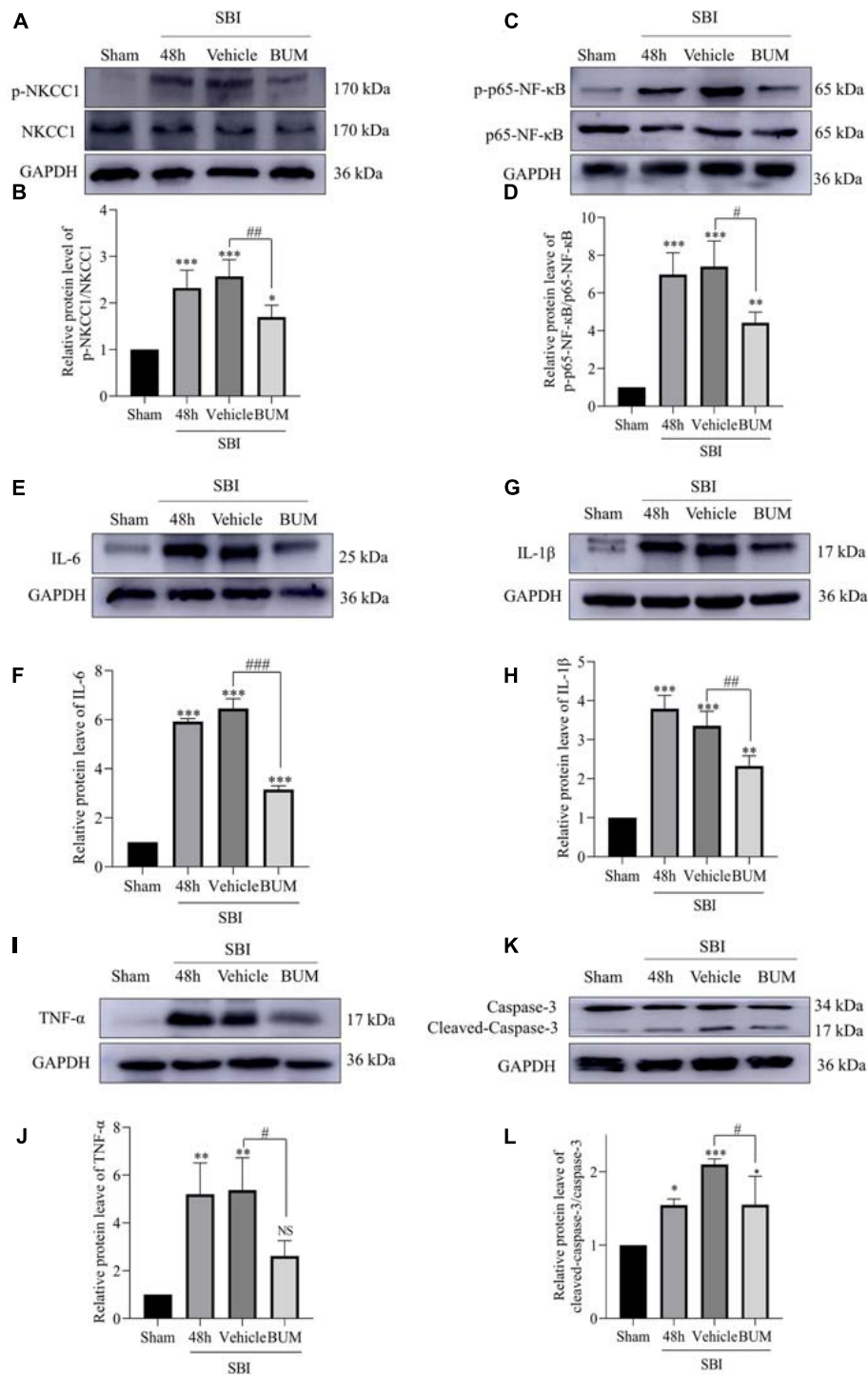


**FIGURE 5** | Expression levels of related proteins after the intervention of BUM 48 h after SBI. The protein-expression levels of p-NKCC1 (**A,B**), p-p65-NF- $\kappa$ B (**C,D**), IL-6 (**E,F**), IL-1 $\beta$  (**G,H**), TNF- $\alpha$  (**I,J**), and caspase-3 (**K,L**) were assessed to determine the effect of BUM intervention on peripheral cortex injury 48 h post SBI. Statistical analyses were performed by a K-W one-way ANOVA followed by the Student–Newman–Keuls *post hoc* test.  $n = 4$  for each group. \*\* $P < 0.01$ , \*\*\* $P < 0.001$  compared to the sham group. # $P < 0.05$ , ## $P < 0.01$ , ### $P < 0.001$  compared to the SBI + vehicle group.

group, TNF- $\alpha$  expression in the SBI group and SBI + vehicle group significantly increased. After intervention by BUM, WB showed significantly lower TNF- $\alpha$  expression in the SBI + BUM

group compared with the SBI + vehicle group (**Figures 5I,J**). The trend for caspase-3, IL-1 $\beta$ , and IL-6 were roughly the same as that of p-p65-NF- $\kappa$ B (**Figures 5E–H,K,L**). These results

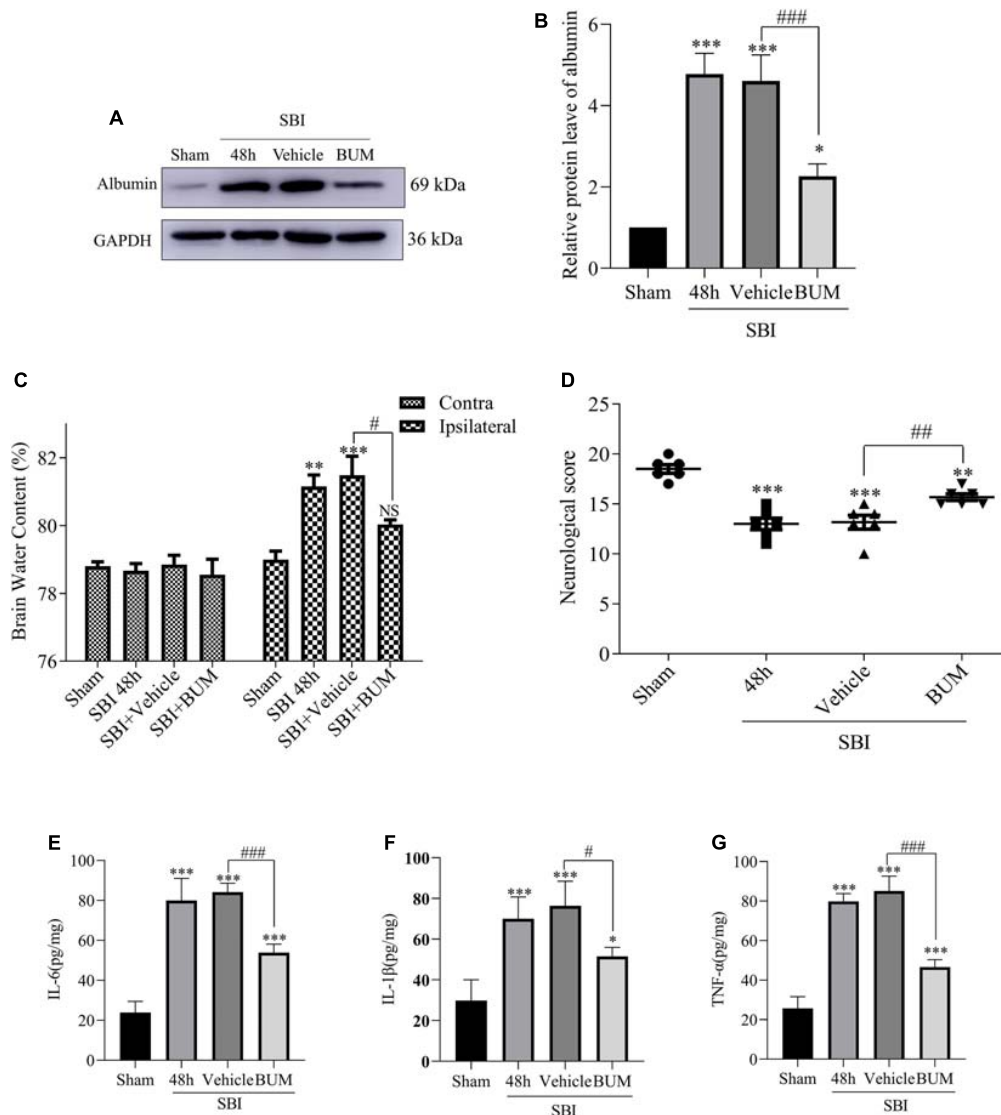


**FIGURE 6 |** Effect of BUM intervention on ELISA, brain edema and neurological score 48 h after SBI surgery. The protein expression levels of albumin (**A,B**) were measured to evaluate the effect of BUM intervention on peripheral cortex injury 48 h after SBI. Brain water content of the bilateral hemispheres of the study groups was determined using the wet-dry method (**C**). Neurological behavioral scores in the SBI rats after BUM intervention (**D**). The ELISA expression levels of IL-6 (**E**), IL-1 $\beta$  (**F**) and TNF- $\alpha$  (**G**) were assessed to determine the effect of BUM intervention on peripheral cortex injury 48 h after SBI. Statistical analyses were conducted using a K-W one-way ANOVA and the Student-Newman-Keuls *post hoc* test.  $n = 4$  for each group. \*\* $P < 0.01$ , \*\*\* $P < 0.001$ , compared with the sham group. # $P < 0.05$ , ## $P < 0.01$ , ### $P < 0.001$ , compared with the SBI + Vehicle group.

confirmed that after SBI, inflammatory factors were released in large quantities, neuroinflammation was aggravated, and inflammation significantly improved after BUM intervention.

### ELISA, Brain Edema, and Neurological Behavioral Scores in SBI Rats After BUM Intervention

Compared with the sham group, albumin expression in the SBI group and SBI + vehicle group and SBI + BUM group significantly increased. After BUM intervention, WB showed lower albumin expression in the BUM group compared with

the SBI + vehicle group (**Figures 6A,B**). In addition, after SBI, cerebral edema in damaged hemispheres was significantly reduced by BUM intervention. However, there was no significant change in cerebral edema lateral to the SBI site of injury compared with the sham group (**Figure 6C**). Neurological scores of the SBI and SBI + vehicle groups were significantly lower than the sham group. Compared with the SBI + vehicle group, the neurobehavioral scores of the SBI + BUM group significantly improved. These results indicate that neurobehavioral scores significantly improved after SBI + BUM intervention (**Figure 6D**). ELISA was detected, compared with the sham group, IL-1 $\beta$ , IL-6, and TNF- $\alpha$  expression in the SBI

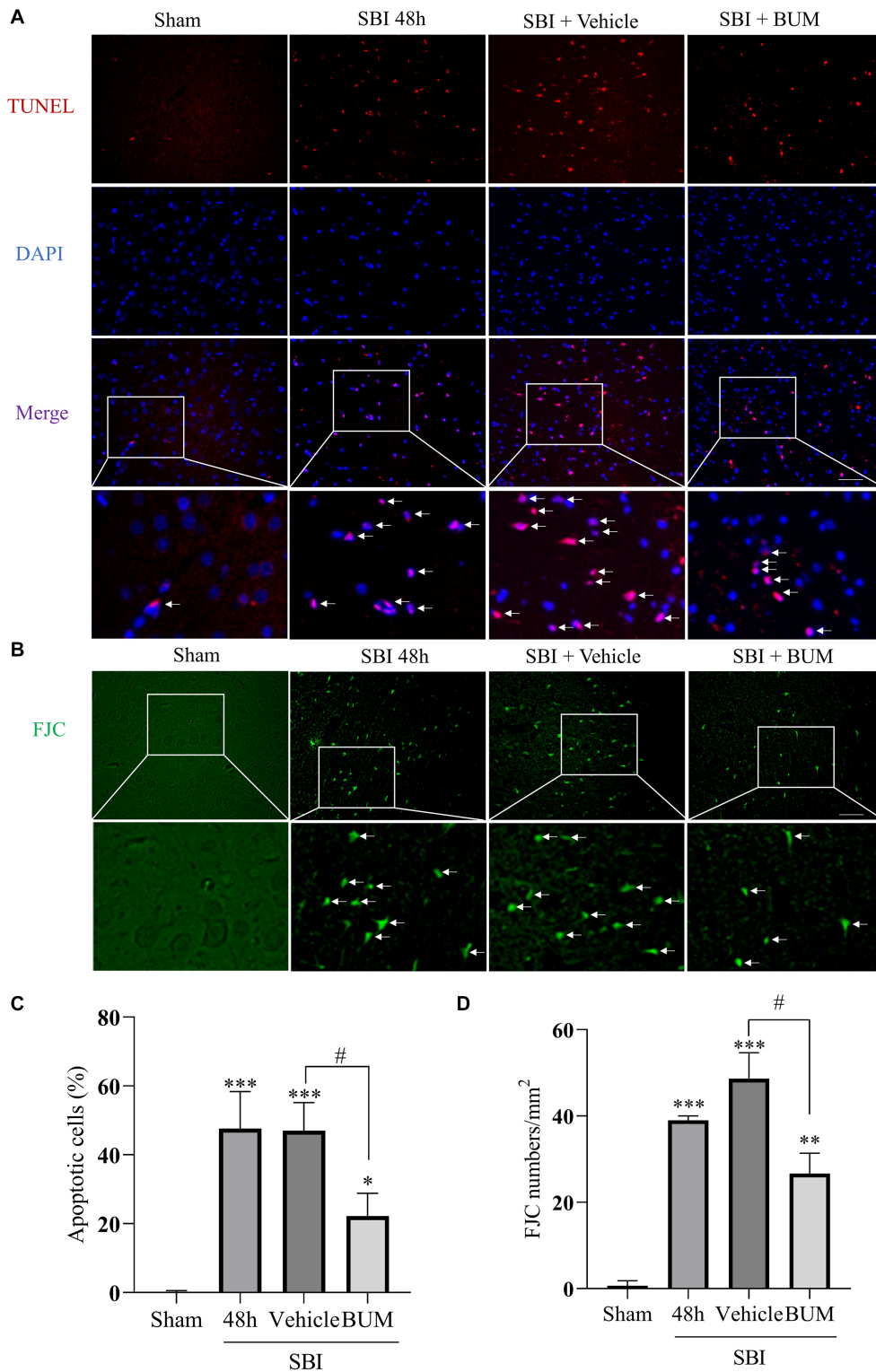
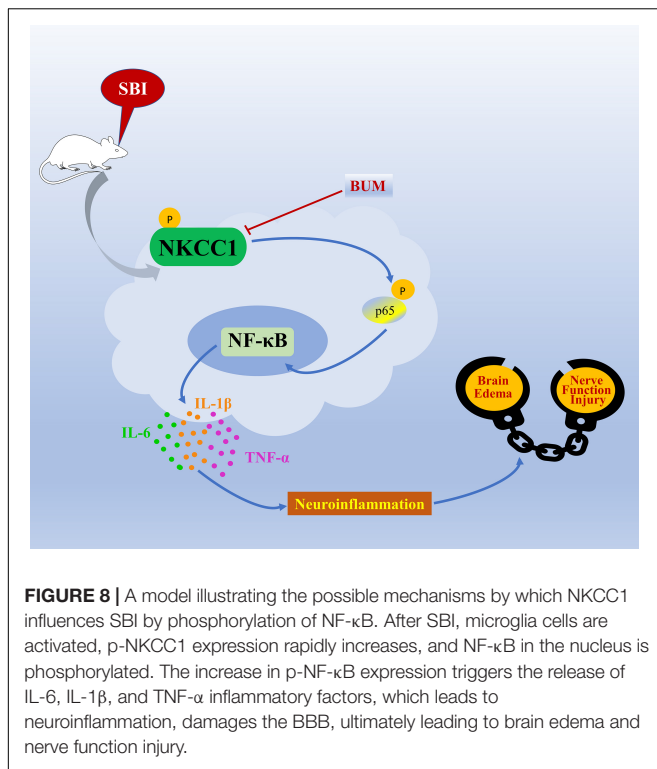


**FIGURE 7** | Effects of BUM intervention on peripheral cortical cell degeneration and apoptosis 48 h after SBI. Neuronal apoptosis was assessed by TUNEL staining (**A,C**). TUNEL (red) labeled apoptosis and DAPI (blue) labeled nuclei. FJC (green) staining detected cell denaturation (**B,D**). Scale bar = 50  $\mu$ m. Statistical analysis was conducted using K-W one-way ANOVA, then with a Student–Newman–Keuls *post hoc* test.  $n = 4$  for each group. \*\* $P < 0.01$ , \*\*\* $P < 0.001$ , compared with the sham group. # $P < 0.05$ , compared with the SBI + vehicle group.





and SBI + vehicle groups significantly increased. After BUM intervention, ELISA showed significantly lower IL-6 (**Figure 6E**), IL-1 $\beta$  (**Figure 6F**), TNF- $\alpha$  (**Figure 6G**) expression levels in the BUM group compared with the SBI + vehicle group.

### Effect of BUM Intervention on Neuronal Apoptosis and Degeneration Post SBI

The extent of apoptosis and neuronal degeneration in the SBI group and SBI + vehicle group and SBI + BUM group were marked higher than the sham group; however, no significant differences in these parameters were observed between the SBI and SBI + vehicle groups. Additionally, the extent of degeneration and apoptosis in the SBI + BUM group significantly decreased compared to the SBI + vehicle group (**Figure 7**).

## DISCUSSION

In this study, we investigated the neuroprotective effect of inhibiting NKCC1 in the SBI rat model and explored its potential mechanism. Our study showed that NKCC1 expression did not show any significant changes after SBI, and p-NKCC1 protein levels began to rise 12 h after SBI and peaked at 48 h (**Figure 2**), subsequently decreased, and basically returned to normal levels on the 7th day. This suggested that NKCC1 plays a role via phosphorylation rather than inducing a total increase in the rat SBI model. This result is concordant to the findings of a previous study (Wu et al., 2020a). We found that BUM inhibition of NKCC1 can reduce the phosphorylation of NF- $\kappa$ B, reduce the release of inflammatory factors (IL-1 $\beta$ , IL-6, and TNF- $\alpha$ ),

reduce degeneration and apoptosis of nerve cells around the damaged area, improve nerve function, and reduce brain edema (**Figures 4–7**). This suggested that the brain edema and neuronal apoptosis after SBI were mediated by the activation of the NKCC1/NF- $\kappa$ B signaling pathway.

Microglia are considered to be the macrophages of the central nervous system, involved in chronic inflammation. The inflammation induced by the immune response is an important factor of neuron death after brain injury (Liu and Hong, 2003). In the early brain injury, the microglia can produce proinflammatory medium (IL-1 $\beta$ , IL-6, TNF- $\alpha$ ), nerve toxicity compounds, reactive oxygen species, nitric oxide and other harmful substances (Chen et al., 2015; Wu et al., 2017a). At present, the mechanism by which microglia regulate the release of inflammatory cytokines after SBI is not fully understood. Increasing evidence shown that the upregulated expression levels of NKCC1 and inflammatory mediators including IL-1 $\beta$ , IL-6, and TNF- $\alpha$  were closely related to the development of secondary brain injury (Huang et al., 2014). Study have shown that inhibition of NKCC1 in microglia can reduce NF- $\kappa$ B and thus reduce inflammation after TBI (Zhang et al., 2017). Our study found that p-NKCC1 and p-NF- $\kappa$ B expression in microglia were significantly increased after SBI, leading to increased release of inflammatory factors such as IL-1 $\beta$ , IL-6, and TNF- $\alpha$  by microglia. After BUM intervention, p-NKCC1 in microglia cells was decreased, suggesting that BUM could inhibit the activity of NKCC1 in microglia cells. Moreover, p-p65-NF- $\kappa$ B was also reduced in microglia, which suggested that NF- $\kappa$ B was at least partially regulated by NKCC1 in SBI rat models (**Figures 4, 5**). NF- $\kappa$ B has been recognized as a central mediator of inflammatory processes and a key participant in innate and adaptive immune responses (DiDonato et al., 2012). By detected NF- $\kappa$ B signaling and downstream inflammatory cytokines, we found that reduction of p-p65-NF- $\kappa$ B inhibited the release of inflammatory cytokines in microglia. Inflammation damages the central nervous system, leading to an increase in apoptotic nerve cells (Takahashi et al., 2005). Under normal physiological conditions of brain tissue, microglia cells are dormant. After brain injury, microglia are activated and release inflammatory cytokines IL-1 $\beta$ , IL-6, and TNF- $\alpha$  (Huang et al., 2020b). This allows inflammatory substances to leak into the brain parenchyma, causing widespread neuroinflammation, leading to brain edema, and impaired nerve function (Haruwaka et al., 2019). Our study has shown that after SBI, microglia cells release a large number of inflammatory cytokines, causing neuroinflammation, leading to degeneration and increased apoptosis of nerve cells around the brain damaged area. Large amounts of nerve cell apoptosis can result in impaired nerve function. In addition, the apoptosis of nerve cells can destroy the BBB and aggravate the secondary brain edema after SBI.

Na<sup>+</sup>-K<sup>+</sup>-Cl<sup>-</sup> cotransporter 1 (NKCC1) belongs to the cation-Cl<sup>-</sup> Cotransporters and is an important determinant of ion homeostatics in brain. In the central nervous system, intracellular chloride concentrations are determined by NKCC1 and KCC2, and the two chloride ion channels have been identified as novel targets for the treatment of cerebral edema (Lee et al., 2003; Tian et al., 2015). By phosphorylating NKCC1, ions flow into the cell.

Coordination across membrane ion and water flow of microglia and other nerve cells in the volume of the steady state is also necessary. As an ion regulatory protein, NKCC1 regulates of cell permeability changes (Matchett et al., 2006). In this study, we found that the expression of albumin and brain water content increased in the rat SBI model several hours post SBI. In fact, this may be due to the increase in p-NKCC1, which regulates the entry of substances such as  $\text{Na}^+$ ,  $\text{K}^+$ ,  $\text{Cl}^-$ , and water into cells, change cell volume, and destroy the cytoskeletal structure of cells, leading to cell swelling, increased BBB permeability, and albumin leakage, ultimately resulting in brain edema. NKCC1/NF- $\kappa$ B signaling affected secondary brain injury after SBI by regulating inflammation. Activation of this signaling pathway promoted microglia to release a large number of inflammatory mediators. At the same time, p-NKCC1 could open the channels on the cell membrane, increase the cell volume, and expand the space between the cell membranes. This promoted the transport of inflammatory cytokines, lead to swelling and apoptosis of cell, destructed of BBB, aggravated of brain edema. Our study showed that after inhibiting p-NKCC1, compared with the injured group, albumin exudation, cerebral water content, and inflammatory factors of the injured side of rats with cerebral edema as well as apoptosis significantly decreased (Figure 7). These results suggest that inhibiting p-NKCC1 can reduce neuroinflammation in SBI rats, protect BBB, and improve the apoptosis of nerve cells, thereby reducing SBI-induced brain edema and imparting a protective role in the brain.

The mechanism of SBI causing secondary brain injury is highly complex. According to our research, p-NKCC1 in microglia increased greatly after SBI, and the phosphorylation of downstream p-p65-NF- $\kappa$ B signal increased accordingly. Microglia cells are activated and release a large number of inflammatory factors, leading to neuroinflammation. Meanwhile, as an ion-regulating protein, NKCC1 can increase the volume and permeability and water content of cells, promote the diffusion of inflammatory factors, aggravate inflammation, lead to degeneration and apoptosis of nerve cells, and cause brain edema and neurological dysfunction. Inhibition of NKCC1/NF- $\kappa$ B signaling pathway can alleviate secondary brain injury caused by SBI (Figure 8).

However, this study is limited by the small sample size and use of only male rats. Thus, we were unable to assess gender differences in p-NKCC1 expression after SBI. Furthermore, to further verify our results, we did not study whether upregulation of p-NKCC1 aggravates SBI-induced secondary brain injury. We will continue investigating the above deficiencies in future studies.

## REFERENCES

- Adukauskiene, D., Bivainyte, A., and Radaviciute, E. (2007). [Cerebral edema and its treatment]. *Medicina (Kaunas)* 43, 170–176.
- Akyol, O., Sherchan, P., Yilmaz, G., Reis, C., Ho, W. M., Wang, Y., et al. (2018). Neurotrophin-3 provides neuroprotection via TrkC receptor dependent pErk5 activation in a rat surgical brain injury model. *Exp. Neurol.* 307, 82–89. doi: 10.1016/j.expneurol.2018.06.002

## CONCLUSION

Here, we show that after SBI in rats, NKCC1 is activated, phosphorylates downstream p-p65-NF- $\kappa$ B, and promotes microglia to secrete IL-1 $\beta$ , IL-6, TNF- $\alpha$ , which aggravates secondary brain injury. Inhibiting the activity of NKCC1 induces protective effects on the brain. These results indicate that NKCC1 may be potentially used as a prevention and control target for SBI.

## DATA AVAILABILITY STATEMENT

The original contributions presented in the study are included in the article/supplementary material, further inquiries can be directed to the corresponding authors.

## ETHICS STATEMENT

The animal study was reviewed and approved by the Institute of Animal Care Committee of Zhangjiagang Traditional Chinese Medicine Hospital.

## AUTHOR CONTRIBUTIONS

GC and BD conceived and designed the study. YG and MW conducted the experiment and wrote the manuscript. JS helped in capturing and processing micrographs. JT and JL assisted in the literature search and conducted the statistical analysis. JX reviewed and revised the manuscript. All authors have read and approved the submission of the manuscript.

## FUNDING

This work was supported by the Zhangjiagang Science and Technology Project (ZKS1914), Zhangjiagang Youth Science and Technology Project (ZJGQNKJ202030), and Suzhou “Science, Education, and Health” Youth Science and Technology Project (KJXW2020062).

## ACKNOWLEDGMENTS

We thank LetPub (www.letpub.com) for its linguistic assistance during the preparation of this manuscript.

- Ben-Ari, Y. (2017). NKCC1 chloride importer antagonists attenuate many neurological and psychiatric disorders. *Trends Neurosci.* 40, 536–554. doi: 10.1016/j.tins.2017.07.001
- Chen, J., Chen, G., Li, J., Qian, C., Mo, H., Gu, C., et al. (2014). Melatonin attenuates inflammatory response-induced brain edema in early brain injury following a subarachnoid hemorrhage: a possible role for the regulation of pro-inflammatory cytokines. *J. Pineal Res.* 57, 340–347. doi: 10.1111/jpi.12173

- Chen, S., Yang, Q., Chen, G., and Zhang, J. H. (2015). An update on inflammation in the acute phase of intracerebral hemorrhage. *Transl. Stroke Res.* 6, 4–8. doi: 10.1007/s12975-014-0384-4
- DiDonato, J. A., Mercurio, F., and Karin, M. (2012). NF- $\kappa$ B and the link between inflammation and cancer. *Immunol. Rev.* 246, 379–400. doi: 10.1111/j.1600-065X.2012.01099.x
- Feng, D., Wang, B., Wang, L., Abraham, N., Tao, K., Huang, L., et al. (2017). Pre-ischemia melatonin treatment alleviated acute neuronal injury after ischemic stroke by inhibiting endoplasmic reticulum stress-dependent autophagy via PERK and IRE1 signalings. *J. Pineal Res.* 62:e12395. doi: 10.1111/jpi.12395
- Gharaylou, Z., Shafaghi, L., Oghabian, M. A., Yoonessi, A., Tafakhori, A., Shahsavand Ananloo, E., et al. (2019). Longitudinal effects of bumetanide on neuro-cognitive functioning in drug-resistant epilepsy. *Front. Neurol.* 10:483. doi: 10.3389/fneur.2019.00483
- Gomez, C. D., Read, J., Acharjee, S., and Pittman, Q. J. (2019). Early life inflammation increases CA1 pyramidal neuron excitability in a sex and age dependent manner through a chloride homeostasis disruption. *J. Neurosci.* 39, 7244–7259. doi: 10.1523/JNEUROSCI.2973-18.2019
- Hamard, L., Ratel, D., Selek, L., Berger, F., van der Sanden, B., and Wion, D. (2016). The brain tissue response to surgical injury and its possible contribution to glioma recurrence. *J. Neurooncol.* 128, 1–8. doi: 10.1007/s11060-016-2096-y
- Hampel, P., Romermann, K., Gramer, M., and Loscher, W. (2021). The search for brain-permeant NKCC1 inhibitors for the treatment of seizures: Pharmacokinetic-pharmacodynamic modelling of NKCC1 inhibition by azosemide, torasemide, and bumetanide in mouse brain. *Epilepsy Behav.* 114(Pt A):107616. doi: 10.1016/j.yebeh.2020.107616
- Haruwaka, K., Ikegami, A., Tachibana, Y., Ohno, N., Konishi, H., Hashimoto, A., et al. (2019). Dual microglia effects on blood brain barrier permeability induced by systemic inflammation. *Nat. Commun.* 10:5816. doi: 10.1038/s41467-019-13812-z
- Huang, L., Tang, H., Sherchan, P., Lenahan, C., Boling, W., Tang, J., et al. (2020a). The activation of phosphatidylserine/CD36/TGF- $\beta$ 1 pathway prior to surgical brain injury attenuates neuroinflammation in rats. *Oxid. Med. Cell Longev.* 2020:4921562. doi: 10.1155/2020/4921562
- Huang, L. Q., Zhu, G. F., Deng, Y. Y., Jiang, W. Q., Fang, M., Chen, C. B., et al. (2014). Hypertonic saline alleviates cerebral edema by inhibiting microglia-derived TNF- $\alpha$  and IL-1 $\beta$ -induced Na-K-Cl Cotransporter up-regulation. *J. Neuroinflamm.* 11:102. doi: 10.1186/1742-2094-11-102
- Huang, Y., Chen, S., Luo, Y., and Han, Z. (2020b). Crosstalk between inflammation and the BBB in stroke. *Curr. Neuropharmacol.* 18, 1227–1236. doi: 10.2174/1570159X18666200620230321
- Hung, C. M., Peng, C. K., Wu, C. P., and Huang, K. L. (2018). Bumetanide attenuates acute lung injury by suppressing macrophage activation. *Biochem. Pharmacol.* 156, 60–67. doi: 10.1016/j.bcp.2018.08.013
- Hung, C. M., Peng, C. K., Yang, S. S., Shui, H. A., and Huang, K. L. (2020). WNK4-SPAK modulates lipopolysaccharide-induced macrophage activation. *Biochem. Pharmacol.* 171:113738. doi: 10.1016/j.bcp.2019.113738
- Kharod, S. C., Kang, S. K., and Kadam, S. D. (2019). Off-Label Use of Bumetanide for brain disorders: an overview. *Front. Neurosci.* 13:310. doi: 10.3389/fnins.2019.00310
- Lee, H. A., Jeong, H., Kim, E. Y., Nam, M. Y., Yoo, Y. J., Seo, J. T., et al. (2003). Bumetanide, the specific inhibitor of Na<sup>+</sup>-K<sup>+</sup>-2Cl<sup>-</sup> cotransport, inhibits 1 $\alpha$ ,25-dihydroxyvitamin D<sub>3</sub>-induced osteoclastogenesis in a mouse co-culture system. *Exp. Physiol.* 88, 569–574. doi: 10.1113/eph8802558
- Lima Giacobbo, B., Doorduyn, J., Klein, H. C., Dierckx, R., Bromberg, E., and de Vries, E. F. J. (2019). Brain-derived neurotrophic factor in brain disorders: focus on neuroinflammation. *Mol. Neurobiol.* 56, 3295–3312. doi: 10.1007/s12035-018-1283-6
- Liu, B., and Hong, J. S. (2003). Role of microglia in inflammation-mediated neurodegenerative diseases: mechanisms and strategies for therapeutic intervention. *J. Pharmacol. Exp. Ther.* 304, 1–7. doi: 10.1124/jpet.102.035048
- Lu, K. T., Wu, C. Y., Cheng, N. C., Wo, Y. Y., Yang, J. T., Yen, H. H., et al. (2006). Inhibition of the Na<sup>+</sup>-K<sup>+</sup>-2Cl<sup>-</sup> cotransporter in choroid plexus attenuates traumatic brain injury-induced brain edema and neuronal damage. *Eur. J. Pharmacol.* 548, 99–105. doi: 10.1016/j.ejphar.2006.07.048
- Matchett, G., Hahn, J., Obenaus, A., and Zhang, J. (2006). Surgically induced brain injury in rats: the effect of erythropoietin. *J. Neurosci. Methods* 158, 234–241. doi: 10.1016/j.jneumeth.2006.06.003
- Reid, A. Y., Riaz, K., Campbell Teskey, G., and Pittman, Q. J. (2013). Increased excitability and molecular changes in adult rats after a febrile seizure. *Epilepsia* 54, e45–e48. doi: 10.1111/epi.12061
- Sherchan, P., Huang, L., Akyol, O., Reis, C., Tang, J., and Zhang, J. H. (2017). Recombinant Slit2 reduces surgical brain injury induced blood brain barrier disruption via Robo4 dependent Rac1 activation in a rodent model. *Sci. Rep.* 7:746. doi: 10.1038/s41598-017-00827-z
- Sherchan, P., Huang, L., Wang, Y., Akyol, O., Tang, J., and Zhang, J. H. (2016). Recombinant Slit2 attenuates neuroinflammation after surgical brain injury by inhibiting peripheral immune cell infiltration via Robo1-srGAP1 pathway in a rat model. *Neurobiol. Dis.* 85, 164–173. doi: 10.1016/j.nbd.2015.11.003
- Simard, J. M., Kahle, K. T., and Gerzanich, V. (2010). Molecular mechanisms of microvascular failure in central nervous system injury—synergistic roles of NKCC1 and SUR1/TRPM4. *J. Neurosurg.* 113, 622–629. doi: 10.3171/2009.11.JNS081052
- Sudhakar, S. K., Choi, T. J., and Ahmed, O. J. (2019). Biophysical modeling suggests optimal drug combinations for improving the efficacy of GABA agonists after traumatic brain injuries. *J. Neurotrauma* 36, 1632–1645. doi: 10.1089/neu.2018.6065
- Takahashi, K., Rochford, C. D., and Neumann, H. (2005). Clearance of apoptotic neurons without inflammation by microglial triggering receptor expressed on myeloid cells-2. *J. Exp. Med.* 201, 647–657. doi: 10.1084/jem.20041611
- Tian, Y., Guo, S. X., Li, J. R., Du, H. G., Wang, C. H., Zhang, J. M., et al. (2015). Topiramate attenuates early brain injury following subarachnoid haemorrhage in rats via duplex protection against inflammation and neuronal cell death. *Brain Res.* 1622, 174–185. doi: 10.1016/j.brainres.2015.06.007
- Tsai, T. H., Lin, S. H., Wu, C. H., Tsai, Y. C., Yang, S. F., and Lin, C. L. (2020). Mechanisms and therapeutic implications of RTA 408, an activator of Nrf2, in subarachnoid hemorrhage-induced delayed cerebral vasospasm and secondary brain injury. *PLoS One* 15:e0240122. doi: 10.1371/journal.pone.0240122
- Wang, Y. C., Cui, Y., Cui, J. Z., Sun, L. Q., Cui, C. M., Zhang, H. A., et al. (2015). Neuroprotective effects of brilliant blue G on the brain following traumatic brain injury in rats. *Mol. Med. Rep.* 12, 2149–2154. doi: 10.3892/mmr.2015.3607
- Wu, C. H., Shyue, S. K., Hung, T. H., Wen, S., Lin, C. C., Chang, C. F., et al. (2017a). Genetic deletion or pharmacological inhibition of soluble epoxide hydrolase reduces brain damage and attenuates neuroinflammation after intracerebral hemorrhage. *J. Neuroinflamm.* 14:230. doi: 10.1186/s12974-017-1005-4
- Wu, C. Y., Fang, M., Karthikeyan, A., Yuan, Y., and Ling, E. A. (2017b). Scutellarin attenuates microglia-mediated neuroinflammation and promotes astroglial in cerebral Ischemia - a therapeutic consideration. *Curr. Med. Chem.* 24, 718–727. doi: 10.2174/092986732466616118142045
- Wu, D., Lai, N., Deng, R., Liang, T., Pan, P., Yuan, G., et al. (2020a). Activated WNK3 induced by intracerebral hemorrhage deteriorates brain injury maybe via WNK3/SPAK/NKCC1 pathway. *Exp. Neurol.* 332:113386. doi: 10.1016/j.expneurol.2020.113386
- Wu, D., Zhang, G., Zhao, C., Yang, Y., Miao, Z., and Xu, X. (2020b). Interleukin-18 from neurons and microglia mediates depressive behaviors in mice with post-stroke depression. *Brain Behav. Immun.* 88, 411–420. doi: 10.1016/j.bbi.2020.04.004
- Wu, M. Y., Gao, F., Yang, X. M., Qin, X., Chen, G. Z., Li, D., et al. (2020c). Matrix metalloproteinase-9 regulates the blood brain barrier via the hedgehog pathway in a rat model of traumatic brain injury. *Brain Res.* 1727:146553. doi: 10.1016/j.brainres.2019.146553
- Xiao, Y., Li, G., Chen, Y., Zuo, Y., Rashid, K., He, T., et al. (2018). Milk fat globule-epidermal growth factor-8 pretreatment attenuates apoptosis and inflammation via the integrin- $\beta$ 3 pathway after surgical brain injury in rats. *Front. Neurol.* 9:96. doi: 10.3389/fneur.2018.00096
- Yan, Y., and Merlin, D. (2008). Ste20-related proline/alanine-rich kinase: a novel regulator of intestinal inflammation. *World J. Gastroenterol.* 14, 6115–6121. doi: 10.3748/wjg.14.6115
- Yang, W., Liu, Y., Liu, B., Tan, H., Lu, H., Wang, H., et al. (2016). Treatment of surgical brain injury by immune tolerance induced by intrathymic and hepatic portal vein injection of brain antigens. *Sci. Rep.* 6:32030. doi: 10.1038/srep32030



- Zhang, M., Cui, Z., Cui, H., Wang, Y., and Zhong, C. (2017). Astaxanthin protects astrocytes against trauma-induced apoptosis through inhibition of NKCC1 expression via the NF- $\kappa$ B signaling pathway. *BMC Neurosci.* 18:42. doi: 10.1186/s12868-017-0358-z
- Zhang, R., Liu, C., Li, Y., Chen, L., and Xiang, J. (2020a). Tenacissoside H promotes neurological recovery of cerebral ischemia-reperfusion injury in mice by modulating inflammation and oxidative stress via TrkB pathway. *Clin. Exp. Pharmacol. Physiol.* doi: 10.1111/1440-1681.13398 [Epub ahead of print].
- Zhang, X. H., Peng, L., Zhang, J., Dong, Y. P., Wang, C. J., Liu, C., et al. (2020b). Berberine ameliorates subarachnoid hemorrhage injury via induction of sirtuin 1 and inhibiting HMGB1/NF- $\kappa$ B pathway. *Front. Pharmacol.* 11:1073. doi: 10.3389/fphar.2020.01073
- Zhao, Y., Huang, G., Chen, S., Gou, Y., Dong, Z., and Zhang, X. (2016). Homocysteine aggravates cortical neural cell injury through neuronal autophagy overactivation following rat cerebral ischemia-reperfusion. *Int. J. Mol. Sci.* 17:1196. doi: 10.3390/ijms17081196

**Conflict of Interest:** The authors declare that the research was conducted in the absence of any commercial or financial relationships that could be construed as a potential conflict of interest.

Copyright © 2021 Gong, Wu, Shen, Tang, Li, Xu, Dang and Chen. This is an open-access article distributed under the terms of the Creative Commons Attribution License (CC BY). The use, distribution or reproduction in other forums is permitted, provided the original author(s) and the copyright owner(s) are credited and that the original publication in this journal is cited, in accordance with accepted academic practice. No use, distribution or reproduction is permitted which does not comply with these terms.